

## Research Paper

# Engineering Bioactive Self-Healing Antibacterial Exosomes Hydrogel for Promoting Chronic Diabetic Wound Healing and Complete Skin Regeneration

Chenggui Wang<sup>1\*</sup>, Min Wang<sup>2\*</sup>, Tianzhen Xu<sup>1</sup>, Xingxing Zhang<sup>3</sup>, Cai Lin<sup>3</sup>, Weiyang Gao<sup>1</sup>, Huazi Xu<sup>1</sup>, Bo Lei<sup>2,4,5</sup>✉, Cong Mao<sup>1</sup>✉

1. Key Laboratory of Orthopedics of Zhejiang Province, Department of Orthopedics, the Second Affiliated Hospital and Yuying Children's Hospital of Wenzhou Medical University, Wenzhou 325027, China
2. Key Laboratory of Shaanxi Province for Craniofacial Precision Medicine Research, College of Stomatology, Xi'an Jiaotong University, Xi'an 710000, China
3. Center of Diabetic Foot, the First Affiliated Hospital of Wenzhou Medical University, Wenzhou 325000, China
4. Frontier Institute of Science and Technology, Xi'an Jiaotong University, Xi'an 710054, China
5. Instrument Analysis Center, Xi'an Jiaotong University, Xi'an 710054, China

\*These authors contributed equally to this work.

✉ Corresponding authors: maocong@wmu.edu.cn (Cong Mao) and rayboo@xjtu.edu.cn (Bo Lei).

© Ivyspring International Publisher. This is an open access article distributed under the terms of the Creative Commons Attribution (CC BY-NC) license (<https://creativecommons.org/licenses/by-nc/4.0/>). See <http://ivyspring.com/terms> for full terms and conditions.

Received: 2018.09.06; Accepted: 2018.11.19; Published: 2019.01.01

## Abstract

**Rationale:** Chronic nonhealing diabetic wound therapy and complete skin regeneration remains a critical clinical challenge. The controlled release of bioactive factors from a multifunctional hydrogel was a promising strategy to repair chronic wounds.

**Methods:** Herein, for the first time, we developed an injectable, self-healing and antibacterial polypeptide-based FHE hydrogel (F127/OHA-EPL) with stimuli-responsive adipose-derived mesenchymal stem cells exosomes (AMSCs-exo) release for synergistically enhancing chronic wound healing and complete skin regeneration. The materials characterization, antibacterial activity, stimulated cellular behavior and *in vivo* full-thickness diabetic wound healing ability of the hydrogels were performed and analyzed.

**Results:** The FHE hydrogel possessed multifunctional properties including fast self-healing process, shear-thinning injectable ability, efficient antibacterial activity, and long term pH-responsive bioactive exosomes release behavior. *In vitro*, the FHE@exosomes (FHE@exo) hydrogel significantly promoted the proliferation, migration and tube formation ability of human umbilical vein endothelial cells (HUVECs). *In vivo*, the FHE@exo hydrogel significantly enhanced the healing efficiency of diabetic full-thickness cutaneous wounds, characterized with enhanced wound closure rates, fast angiogenesis, re-epithelization and collagen deposition within the wound site. Moreover, the FHE@exo hydrogel displayed better healing outcomes than those of exosomes or FHE hydrogel alone, suggesting that the sustained release of exosomes and FHE hydrogel can synergistically facilitate diabetic wound healing. Skin appendages and less scar tissue also appeared in FHE@exo hydrogel treated wounds, indicating its potent ability to achieve complete skin regeneration.

**Conclusion:** This work offers a new approach for repairing chronic wounds completely through a multifunctional hydrogel with controlled exosomes release.

Key words: multifunctional hydrogel, bioactive exosomes, responsive sustained release, diabetic wound healing

## Introduction

Diabetic wounds have become a significant cause of diabetes related amputations, which lead to

high medical cost and poor life quality of patients [1]. Normal wound healing is a complicated biological

process involving three typical phases: inflammation, proliferation and remodeling, which involves many types of cells, cytokines and extracellular matrix (ECM) [2]. Mechanisms underlying poor healing of diabetic wounds are still unclear, yet the reasons for this dread complication of diabetes mainly involves hypoxia, impaired angiogenesis, damage from reactive oxygen species (ROS), and neuropathy, leading to long-time medical burden and compromised life quality of those patients [3]. Conventional clinical treatment of diabetic wounds includes surgical debridement and negative pressure therapy with wound dressings [1, 4]. However, these treatments often seem ineffective for many patients due to impaired cell function around the wound sites [5]. To solve these problems, therapies based on mesenchymal stem cells (MSCs) showed great potential for wound healing due to their ability to recruit cells and release growth factors and proteins, yet problems still arose because of immunological rejection, limited differentiation and proliferation ability, and chromosomal variation of stem cells [6, 7]. Recently, emerging studies showed that transplanted stem cell therapy may exert its function through a paracrine mechanism instead of direct differentiation, particularly by secreting extracellular vesicles [8, 9]. Exosomes are nanosized vesicles (40-150 nm) that are considered as primary secretory products from MSCs and can regulate cell-to-cell communication through transferring the contained mRNAs, miRNAs, and proteins to target cells and facilitate wound healing [6]. Moreover, they are immune-tolerant, have similar biological functions to those of the cells from which they are derived, and can be used as a possible alternative to MSCs therapy [10]. Angiogenesis is a critical factor determining the outcome of diabetic wound healing [2, 11]. Recent studies also showed that exosomes could improve wound healing by speeding up angiogenesis, which exhibited great promises for diabetic wound therapy application [12, 13]. For example, Guo et al. reported that exosomes derived from platelet-rich plasma can promote chronic cutaneous wound healing through YAP activation [14]. However, the common method of exosomes administration is injection, which can affect their function due to the rapid clearance rate [15]. On the other hand, diabetic wound repair and regeneration require a relatively long healing time. Herein, it is necessary to develop a novel biocompatible scaffold that can serve as a sustained release carrier for exosomes to maintain their bioactivity at the diabetic wound area and further accelerate wound healing.

Biomedical hydrogels, structurally similar to the natural ECM, have been considered promising

biomaterials to deliver drugs/cells for wound treatments [16, 17]. An ideal wound-healing hydrogel scaffold should have these features: appropriate mechanical properties, good water retention, anti-infection capacity, injectable capacity, and excellent cell biocompatibility [18]. Self-healing hydrogels exhibit rapid and autonomous self-recovery ability after damage caused by external forces, possibly maintaining their structural stability during the wound healing [19, 20]. Hydrogels with inherent antibacterial activity possess several advantages such as preventing infection, absorbing wound fluid and offering gaseous exchange [21]. Current antibacterial materials include inorganic metal ions or nanoparticles, reactive oxygen species (ROS)-producing molecules, antimicrobial peptides, etc., which also have their own disadvantages such as potential cytotoxicity, the limitations of utilization, low productivity and high production costs [22-25]. The injective and adhesive capacities of hydrogels could endow them with good operability and long term attachment on wound during healing [26-28]. In particular, the good cellular biocompatibility plays an important role for hydrogels, which could enhance cell proliferation and differentiation [29]. Hydrogel scaffolds contained amine groups have shown their potential for enhanced biocompatibility and integration with host tissue [30]. Poly- $\epsilon$ -L-lysine (EPL) is natural cationic polypeptide produced from *Streptomyces albulus*, which showed good biodegradability, inherent antibacterial activity and biocompatibility [31]. The US FDA has approved EPL for clinical uses or as a food-grade cationic antimicrobial [32]. Furthermore, the L-lysine residues in EPL enabled their facile surface modification to synthesize biomedical hydrogels. For example, EPL and poly(ethylene glycol) hydrogel with adhesive property has been fabricated for potential tissue regeneration applications [33]. On the other hand, exosome-based delivery by hydrogel probably will enhance the angiogenesis and tissue formation during wound healing. Recent studies also showed the use of hydrogels to deliver exosomes for restoring vascularization and promoting wound healing [34, 35]. Chitosan-based hydrogels loaded with exosomes have been developed for accelerating angiogenesis and wound healing [33]. However, hydrogels composed of natural polypeptides with multiple functions for exosome delivery and tissue regeneration were very rare in reports [36]. Therefore, it is very necessary and promising to fabricate an injectable self-healing and adhesive hydrogel with inherent antibacterial activity for delivering exosomes to promote chronic diabetic wound healing.

In this study, we developed an injectable

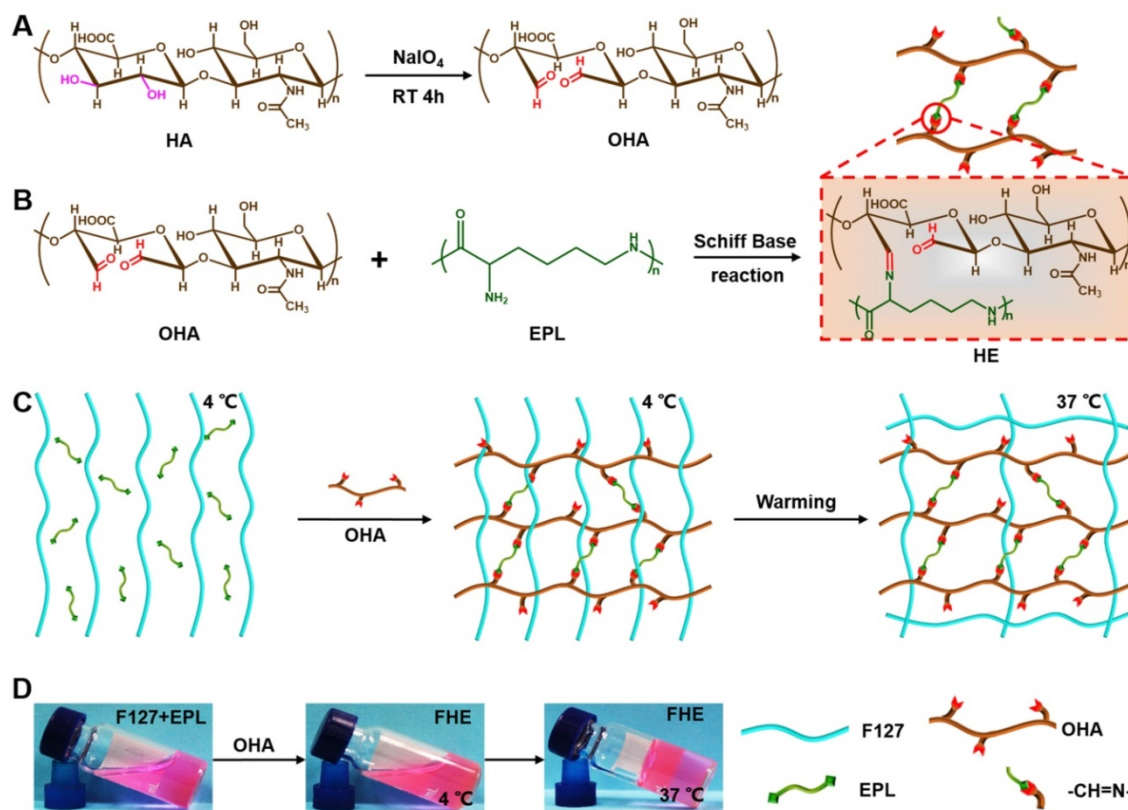
self-healing polypeptide-based hydrogel that exhibited inherent antibacterial activity and pH-responsive long-term exosomes release (Scheme 1). The multifunctional hydrogel was composed of Pluronic F127 (F127), oxidative hyaluronic acid (OHA), and EPL (denoted as FHE hydrogel). The FHE hydrogel was formed through a reversible Schiff base reaction between OHA and EPL, and the thermal-responsive property of F127 (Scheme 1B). In this hydrogel, OHA provides the water-retaining ability and biocompatibility, EPL gives the intrinsic antibacterial activity and adhesive ability, F127 offers the thermal-responsive gelation, and Schiff base bonds (OHA and EPL) endow the self-healing performance. The adipose mesenchymal stem cells (AMSCs)-derived exosomes exhibit representative negative potential and could be loaded in the hydrogel through the electrostatic interaction between exosomes and EPL. The exosomes could be released under a weak acidic environment due to the broken of Schiff base bonds. Herein, for the first time, we reported that the self-healing multifunctional FHE hydrogel could be used to deliver bioactive exosomes for enhancing diabetic wound healing and skin regeneration. The effect of long-term exosomes released in the FHE hydrogel on angiogenesis and

diabetic wound healing was studied.

## Results and discussion

### Physicochemical structure characterization of FHE hydrogel

The schematic representation of the FHE hydrogels is shown in Scheme 1. First, the aldehyde groups were introduced to HA through oxidation by sodium periodate (Scheme 1A). Oxidized HA was identified by  $^1\text{H}$  NMR, in which the new peaks at 4.9 ppm and 5.0 ppm corresponded to protons from the aldehyde group and adjacent hydroxyls (Figure S1). The actual oxidation degree of HA was quantified by measuring the number of aldehydes groups in the polymer using a hydroxylamine hydrochloride assay, and the results are shown in Table S1. Oxidized hyaluronic acid (OHA) can react with amino groups in EPL to form Schiff bases (Scheme 1B). When mixing the F127 and EPL solution with the OHA solution, the mixed solution forms the hydrogels (100  $\mu\text{l}$ ) through a sol-to-gel transition in approximately 10 s at 37°C (Schemes 1C-D). The chemical structure of the hydrogels was determined by FT-IR analysis (Figure 1A). The peak at 1660  $\text{cm}^{-1}$  was assigned to the carbonyl ( $-\text{C}=\text{O}$ ) from EPL and HA. The aldehyde



**Scheme 1. Synthesis of injectable FHE hydrogel with multifunctional properties.** (A) Synthesis of oxidized hyaluronic acid (HA); (B) Schiff base reaction between oxidized HA and polypeptide ( $\epsilon$ -poly-L-lysine, EPL); (C) Thermal-responsive sol-gel process of double network hydrogel composed of F127-EPL and oxidized HA; (D) Optical pictures showing the sol-gel transition of FHE hydrogel.

group (-CHO) stretch in oxidized HA (OHA) was found at  $1735\text{ cm}^{-1}$ . The double peaks at  $1467\text{ cm}^{-1}$  and  $1342\text{ cm}^{-1}$  were attributed to the ether bond (-C-O-C-) from F127. The disappearance of the peak at  $1735\text{ cm}^{-1}$  in FHE hydrogel indicated the successful reaction between OHA and EPL. In addition, after freeze-drying, the FHE hydrogel showed a typical 3D porous morphology and the EPL content did not significantly affect the pore structure (Figure 1B).

### Multifunctional properties evaluation of FHE hydrogels

The rheological properties of FHE hydrogel under various conditions were tested to evaluate the mechanical behavior (Figures 1C-F). At  $4^\circ\text{C}$ , the storage modulus ( $G'$ ) was significantly lower than the loss modulus ( $G''$ ) in the F127 and FH groups, suggesting their low viscosity (Figure 1C). However,

for FHE5 and FHE10 groups, the  $G'$  was high compared with  $G''$ , indicating the increased viscosity after adding OHA and EPL (Figure 1C). The significant low modulus at  $4^\circ\text{C}$  (approximately 10 Pa) suggested that various hydrogels should be in the sol state but not the gel state (Scheme 1). The  $G'$  and  $G''$  of all hydrogels were significantly increased with the temperature at 25 and  $37^\circ\text{C}$ , and the  $G'$  was significantly higher than the  $G''$  in all groups, suggesting the hydrogel formation (Figure 1C). In addition, the rheological analysis and macroscopic test were used to evaluate the self-healing performance of the FHE hydrogels, using F127 and FH as controls (Figures 1D-G). When the step strain changed from 1% to 1000%, the  $G'$  for various hydrogels was significantly decreased from  $\sim 10\text{ kPa}$  to several Pa (Figure 1D). After two cycles of step strain, the  $G'$  of the F127 and FH hydrogels showed a

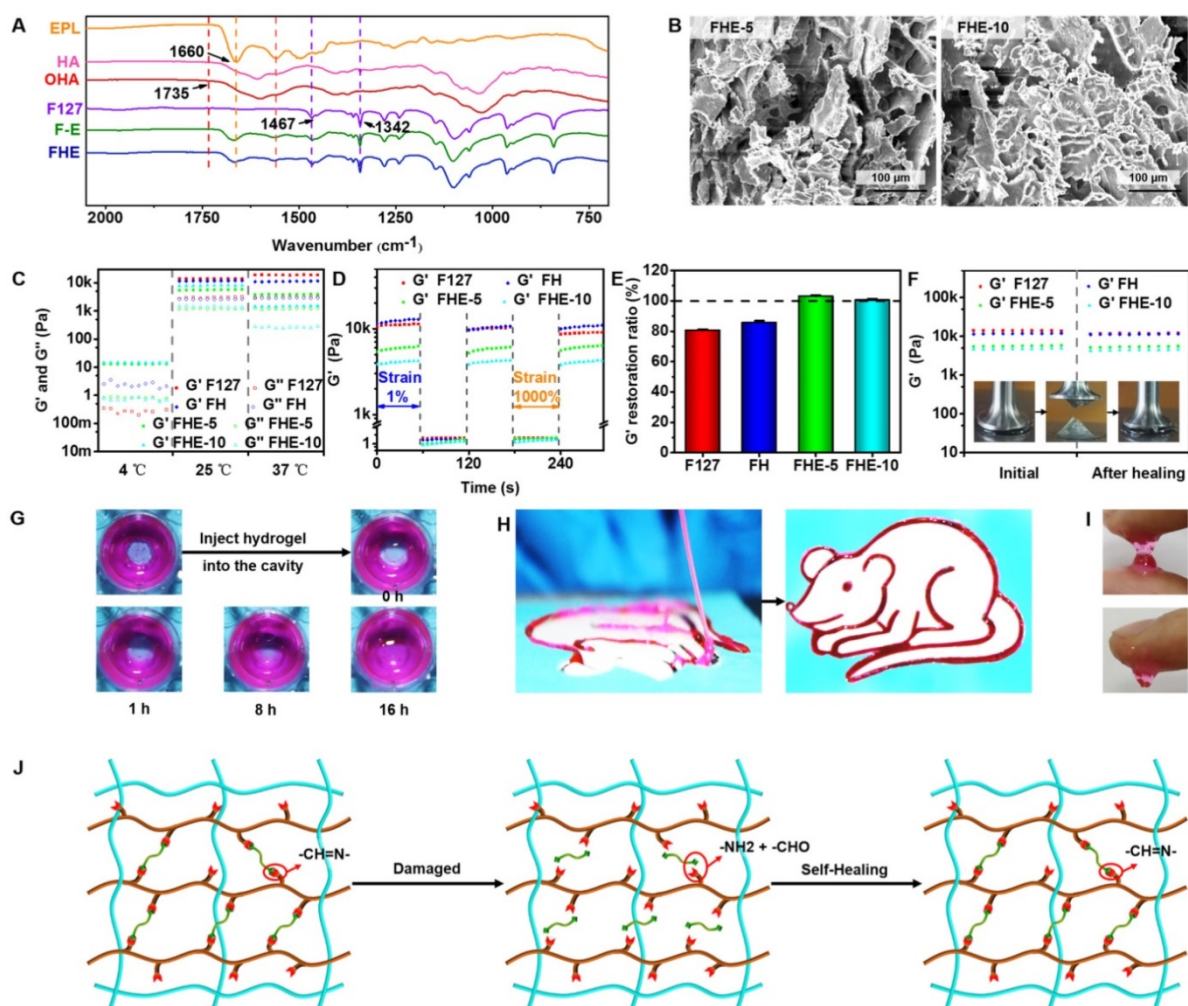


**Figure 1. Physicochemical structure and multifunctional properties of FHE hydrogel.** (A) FTIR showing the chemical structure; (B) SEM images exhibiting the porous morphology; (C) Rheological properties exhibiting the  $G'$  and  $G''$  of various hydrogels at 4, 25 and  $37^\circ\text{C}$ ; (D)  $G'$  and  $G''$  of various hydrogels when the step strain switched from 1% to 1000% at  $37^\circ\text{C}$ ; (E)  $G'$  recovery ratio of various hydrogel after two cycles of 1000% step strain at  $37^\circ\text{C}$ ; (F)  $G'$  of the initial hydrogel and the hydrogel after healing; (G) Pictures demonstrating the self-healing performance of FHE-5 hydrogels; (H) Photographs showing the injectable ability of FHE-5 hydrogel through the catheter; (I) Images presenting the adhesive characteristic to the skin for FHE-5 hydrogel; (J) Schematic illustration of the self-healing process for FHE hydrogel.

significant decrease, while those of the FHE-5 and FHE-10 hydrogels presented a negligible change (Figure 1E). The decrease in  $G'$  was caused by the collapse of the hydrogel network due to the high dynamic strain (1000%). After releasing the strain to 1%, the FHE-5 and FHE-10 hydrogels returned to their initial  $G'$  values quickly, suggesting the recovery of their hydrogel structure (Figures 1D-E and Figure S2A-D). We also tested the rheological properties of hydrogels before and after healing (Figure 1F). No significant difference can be found in  $G'$  between the FHE-5 and FHE-10 hydrogels, indicating their fast recovery ability (Figure S2E). After adding new hydrogel to the defect in hydrogel, the FHE-5 hydrogel repaired the defect within 16 h (Figure 1G), and no significant difference was observed in the rheological properties and structure between the initial and after healing hydrogel (Figure S2G and S2K). Additionally, the FHE-5 hydrogel could be extruded through a medical plastic catheter with an 0.8 mm of inner diameter and 10 cm of length without clogging and recover the gel state in a “rat” shape after injection, indicating its good injectability (Figure 1H). The injectability of FHE hydrogel was also characterized in its the shear thinning properties (Figure S2F). FHE-5 hydrogel also exhibited very good adhesive ability on skin, which may benefit the wound healing process (Figure 1I). The mechanism of the self-healing hydrogel probably was based on the dynamic Schiff based bond (Figure 1J and S2H-J) [37, 38]. Due to the presence of the antibacterial polypeptide (EPL), the FHE hydrogel demonstrated robust antibacterial activity (Figure S3). Compared with the F127 hydrogel, the FHE hydrogel efficiently killed the *E. coli* (Gram-negative bacterium) (Figures S3A-B) and *S. aureus* (Gram-positive bacterium) just after 2 h of incubation (Figures S3C-D). *E. coli* and *S. aureus* showed a significant increase after incubation with F127-HA (FH), indicating the excellent antibacterial ability of FHE hydrogels. After 13 days, the FHE-5 hydrogel exhibited a representative pH-responsive degradation *in vitro*; the weight residual was approximately 20 % (pH 7.4) and 1 % (pH 5.5), indicating that the FHE-5 hydrogel also has been mostly degraded *in vivo* (subcutaneous) (Figure S4). The multifunctional properties of FHE hydrogel including injectability, self-healing, antibacterial and adhesive activity enable their promising applications in wound healing.

### Exosomes characterization, release profile and HUVECs biocompatibility evaluation *in vitro*

The obtained AMSCs were characterized by flow cytometry analysis for positive expression of CD90 and CD44, and negative expression of CD45 and

CD34 (Figure 2). The AMSCs-derived exosomes were then harvested by differential centrifugation of the AMSCs conditioned media. TRPS analysis, TEM, and western blotting were performed to identify the purified exosomes. The TRPS measurement showed that the size of the AMSCs-derived exosomes was approximately 60-80 nm (Figure 2A), which was concordant with the previously reported exosomes size distributions [39]. TEM revealed that AMSCs-derived exosomes exhibited a cup- or round-shaped morphology with a size below 100 nm (Figure 2B), which was consistent with the data from the TRPS analysis. Western blotting indicated that these exosomes were positive for the characteristic exosome surface marker proteins, including Alix, CD9, CD63 and CD81 (Figure 2C), which was also described by other studies [15, 40]. All these results indicated that the AMSCs-derived exosomes were successfully obtained in this study.

The exosomes release profile is shown in Figures 3 A and B. The bioactive exosomes were effectively encapsulated in the FHE hydrogel and exhibited a representative long term pH-responsive sustained release behavior. To investigate the angiogenic ability of AMSCs-derived exosomes, transwell coculture system was used. The function of free exosomes or FHE@exo hydrogels on HUVECs proliferation was tested by CCK-8 cell counting analysis. The results showed that HUVECs treated with FHE hydrogel showed equal proliferative capability to that of the control groups, but the sustained release of exosomes from FHE hydrogel can significantly enhance the proliferation of HUVECs over that of the free exosomes groups (Figure 3C). This result suggested that the FHE hydrogel possessed good biocompatibility and non-cytotoxicity towards HUVECs. Moreover, the sustained release of exosomes from the FHE hydrogel could remarkably enhance the proliferation of HUVECs than one-time treatment of exosomes, indicating that the FHE hydrogel can increase or at least maintain the bioactivity of released exosomes and can be an excellent carrier for the sustained release of exosomes.

Angiogenesis is the biological process of new vessel formation involved in endothelial cell proliferation, migration, and tube formation, which can determine the outcomes of diabetic wound healing because newly formed vessels can transport oxygen and nutrition into wound sites [2, 41]. To evaluate the effect of FHE@exo hydrogel on migration and tube formation of HUVECs, exosomes or FHE@exo hydrogel pretreated HUVECs were seeded on the chamber of the transwell or Matrigel. The total migrated cells and tube numbers were counted to assess the angiogenic ability of HUVECs. As shown in

Figures 3 D and E, exosomes remarkably enhanced the motility of HUVECs compared to that of the control, and this effect on HUVECS was increased with the treatment of FHE@exo hydrogel. Furthermore, better tube formation performance was observed in FHE@exo hydrogel group, characterized with higher tube numbers and complete tubular structure when compared to the FHE hydrogel or exosome alone groups (Figures 3 F and G). This observed phenomenon indicated the sustained release of exosomes could exert a potent effect on angiogenesis, which also confirmed the previous research that exosomes can accelerate angiogenesis and promote wound healing [13, 42, 43]. Herein, the above *in vitro* results showed that AMSCs-derived exosomes activate a cascade of angiogenic responses in HUVECs, including cell proliferation, migration and angiogenic activities, and the sustained release of exosomes from the FHE hydrogel further enhanced the angiogenic ability of HUVECs.

### Diabetic wound healing examinations *in vivo*

To explore the healing efficiency of FHE@exo hydrogel on the cutaneous wound repair process, FHE@exo hydrogel, exosomes and FHE hydrogel were applied to the full-thickness diabetic wounds

and saline were used as the blank control. Figure 4A exhibits the size change of the diabetic wounds from four groups on days 0, 3, 7, 14, and 21 postsurgery. Gross observation of wound closure in mice showed that all treated wounds achieved a remarkable decrease in wound size at 14 and 21 days, while the negative control exhibited a slow decrease of wound size during the experimental time. Among them, the FHE@exo hydrogel possessed the most efficient healing with complete closure and hair growth of diabetic wounds at day 21. Consistent with the gross observation, the quantitative wound closure rates showed that the FHE@exo hydrogel group exhibited faster healing rates than those of other groups during the whole healing process with  $88.67 \pm 6.9\%$  closure rate on day 14, while other groups reached final healing rates of  $76.3 \pm 3.2\%$  (exosomes),  $64.3 \pm 9.8\%$  (FHE hydrogel) and  $36.3 \pm 10.4$  (control), respectively (Figure 4B). Moreover, with the loading of exosomes into the FHE hydrogel, the healing performance of the FHE@exo hydrogel was obviously promoted when compared with the pure exosomes, indicating that the FHE@exo hydrogel can promote the wound healing process through sustained release of exosomes.

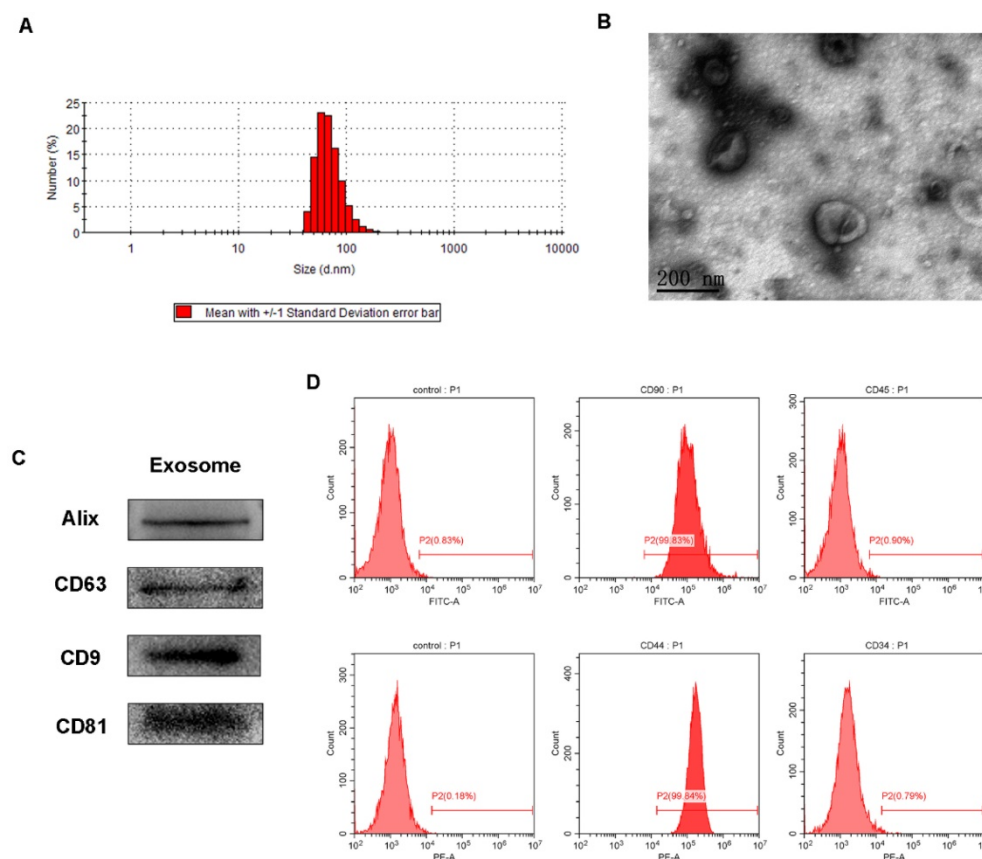


**Figure 2. Characterization of AMSCs and AMSCs-exo.** (A) Size distribution of AMSCs-exo; (B) TEM micrograph of AMSCs-exo, scale bar: 200 nm; (C) Western blot analysis of AMSCs-exo markers of Alix, CD63, CD9 and CD81; (D) flow cytometry analysis of AMSCs markers of CD90, CD34, CD44 and CD45; n=3 independent experiments.

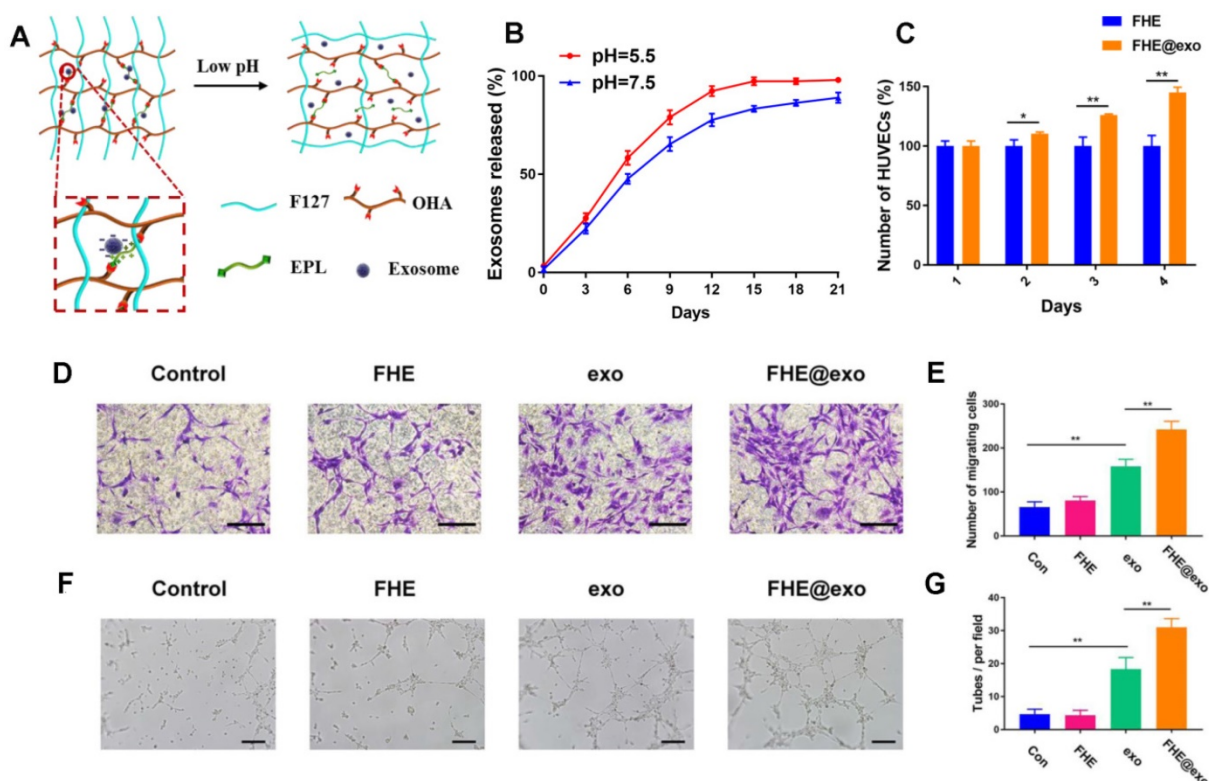


**Figure 3. Exosomes release and HUVECs biocompatibility evaluation *in vitro*.** (A) Scheme of pH- responsive exosomes release in FHE hydrogel; (B) pH-dependent release profile of loaded exosomes in FHE hydrogel; (C) CCK8 results of HUVECs treated by FHE or FHE@exo hydrogels; (D, E) Transwell migration assay results of HUVECs with different treatments. HUVECs were treated with PBS (control), FHE, exosomes and FHE@exo, and the cell migration of HUVECs was enhanced after exosomes or FHE@exo treatment (scale bar: 50  $\mu$ m); (F, G) *In vitro* tube formation results of HUVECs with different treatments. The tube formation ability of HUVECs was improved after exosomes or FHE@exo treatment (scale bar: 200  $\mu$ m).

H&E staining was then used to assess the healing pathology of FHE@exo hydrogel treated wounds. As shown in Figure 4C, unlike the control group, which exhibited with no formed neoepidermis, abundant granulation tissue formed with thicker and more layers in the wound gap of FHE@exo hydrogel, pure exo and FHE hydrogel groups at day 7. The calculated length of wound area also showed a significant difference between FHE@exo and other groups, with the shortest ones in FHE@exo hydrogel group, followed by pure exosomes, FHE hydrogel and control, respectively (Figures 4C, 3D). At day 14, the thickness of granulation tissue was much higher than that at day 7. Although a noticeable reduction in the wound length was also observed in all groups when compared to day 7, FHE@exo hydrogel treated wounds exhibited with the most abundant granulation tissue and shortest wound length (Figure 4E). Moreover, skin appendages were clearly observed at day 21 in the FHE@exo hydrogel group with a significantly higher number of dermal appendages (Figures 4C and F) in the scar tissue when compared with other groups, indicating that complete skin repair can be achieved by the FHE@exo hydrogel treatment. It should also be mentioned that despite the fact that pure exosomes can be useful for wound

healing, the long-time release of exosomes from FHE@exo hydrogel can be more efficient on diabetic wound repair and regeneration from the H&E staining analysis.

### Collagen deposition analysis *in vivo*

Proper collagen deposition and remodeling could improve the tissue tensile strength and result in better healing effect [44, 45]. Figure S5 exhibits the deposition of newly formed collagen in wounds treated by different methods. We can see wounds treated by FHE@exo hydrogel and exosome showed abundant and relatively well-organized collagen fibers at day 7, and the amount of collagen fibers increased with healing time, characterized by abundant well-arranged fibers appearing in the wound site. The FHE hydrogel group showed less collagen, and collagen deposition in control wounds can be hardly seen at day 7 and still had a lower level and loosely packed of collagen fibers when compared with others at day 21. Particularly, FHE@exo hydrogel treated wounds completely healed and skin appendages can be clearly seen at day 21, and this outcome was consistent with the H&E results (Figures 4C and F). Masson staining results suggested that FHE@exo hydrogel, the exosomes sustained release

system, can improve collagen deposition in wound site, resulting in accelerated skin regeneration and better and even complete repair of full-thickness diabetic wounds.

The type I and III collagens are primary constituents in dermal ECM, which is very important in wound healing [46]. Hence, the collagen I/III levels in the wound tissues were evaluated by immunostaining. Figure 5 shows the deposition amount of collagen I and III exhibited similar changing trends to Masson staining. With the increase in healing time, the deposition of both types of collagens also increased in all wounds, while the FHE@exo hydrogel group showed significantly higher intensity (Figures

5A-D) than that of other groups at 7 and 21 days posttreatment, followed by the exosomes, FHE hydrogel and control groups. It is known that scar tissue exhibited relatively lower Col III content than that of normal skin, and early abundant deposition of collagen III would facilitate healing and result in scarless skin [47, 48]. Connecting the pathological results with formed skin appendages and well-organized collagen fibers, the abundant collagen formation during the healing period benefited the collagen matrix remodeling and stimulated complete healing, leading to better healing outcomes with more similar healed tissue to normal skin.

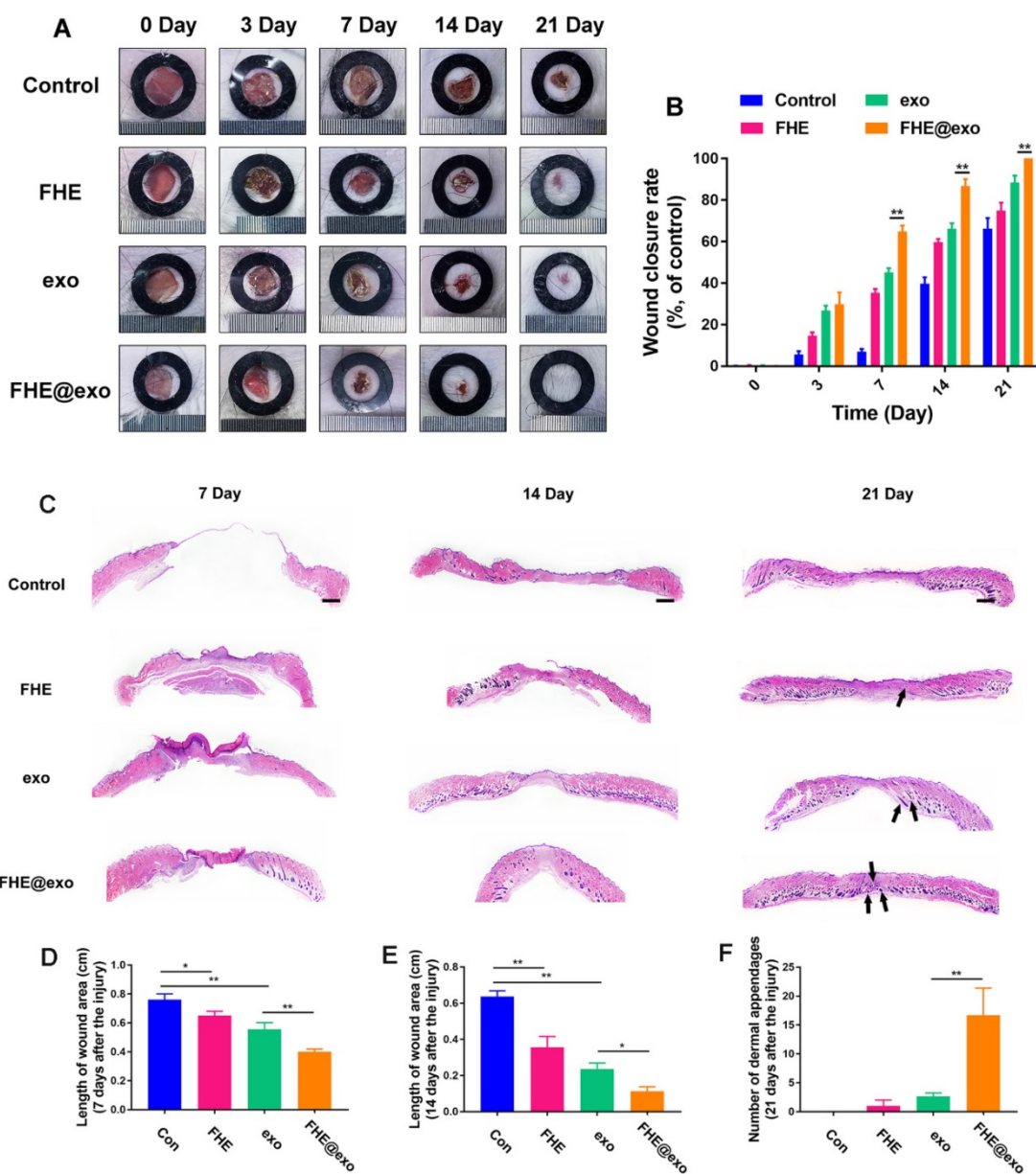


**Figure 4. FHE@Exo hydrogel accelerated wound closure.** (A) Representative images of healing process in wounds treated with FHE, exosomes, FHE@exo and control; (B) Wound closure rates of all four groups; (C) H&E staining images of full-thickness wounds on days 7, 14 and 21, arrows indicate newly formed dermal appendages; (Scale bar: 1000 μm); (D) Quantification of the length of the wound site at day 7; (E) Quantification of the length of the wound area on day 14; (F) Quantification of the number of dermal appendages in the wound area on day 21.



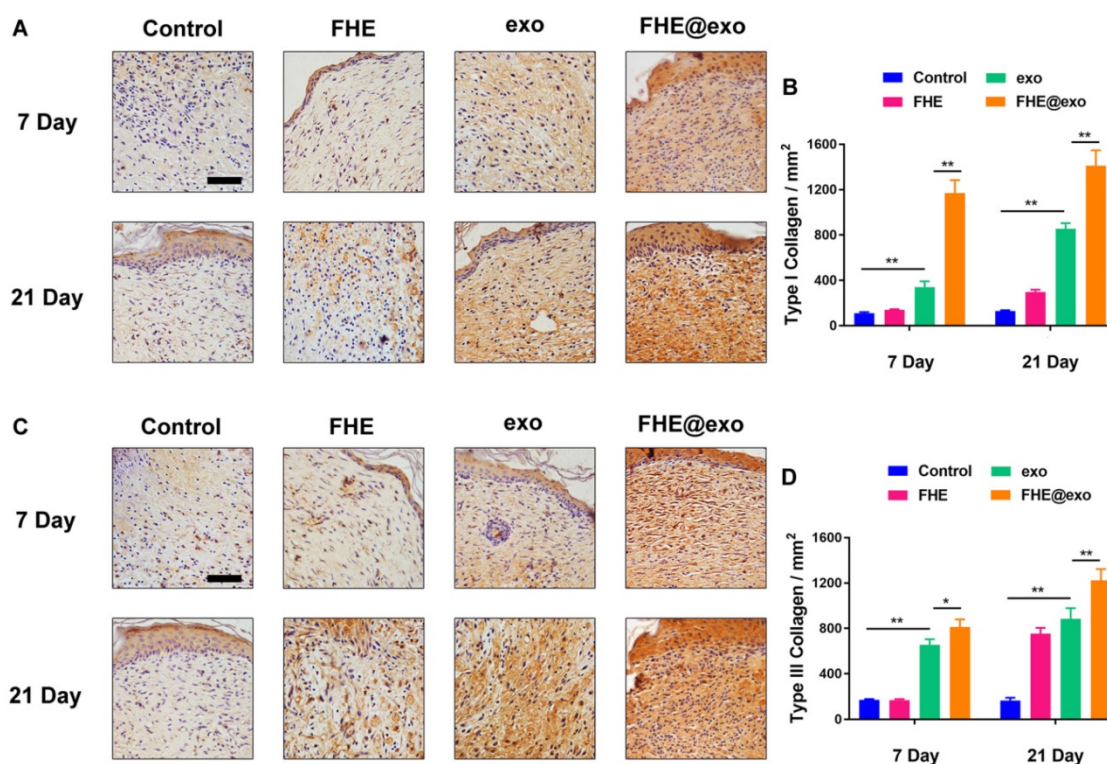


**Figure 5.** Histochemical analysis of collagen I and III expression in wounds treated by FHE@exo hydrogel. (A, C) Immunohistochemistry staining images for collagen I and collagen III at 7 and 21 days post-wounding, respectively; (B, D) Quantitative analysis of relative density of collagen I and collagen III at 7 and 21 days after surgery, respectively; Scale bar: 50  $\mu$ m.

### Re-epithelialization and angiogenic ability assessment *in vivo*

The immunohistochemical staining of cytokeratin, which is a vital biomarker related to the differentiation and re-epithelialization of epidermal [49], was performed to assess the re-epithelialization level during healing. As shown in Figures S6A and B, the FHE@exo hydrogel group exhibited strongest staining of cytokeratin within neopidermis at both day 7 and 14 in comparison to the other groups. FHE@exo hydrogel treated wounds also exhibited the thickest neopidermis with differentiated structures and more well-organized layers (Figure S6A), while control wounds showed significantly lower staining of cytokeratin with less re-epithelialization as observed. Moreover, FHE hydrogel or pure exosomes alone also promoted re-epithelialization of the diabetic wounds, characterized with more positive stained cells with cytokeratin in the neopidermis than those in the control group. This outcome also confirmed that the AMSCs-derived exosomes released into the wound sites promoted the epithelial cell differentiation [42], leading to stronger cytokeratin levels and faster re-epithelialization. The above data suggested that FHE@exo hydrogel, a sustained release system of exosomes, exerted a synergic effect of FHE hydrogel and exosomes, together leading to faster re-epithelialization and wound healing.

The above results revealed that FHE@exo hydrogel can be very efficient for diabetic wound healing through facilitating granulation tissue formation and re-epithelialization during repair. These processes are closely connected to cell activities [44]. In this study, we also evaluate the cell proliferation activities by performing immunostaining of Ki67 at day 7 and 14 (Figure S6C) [50]. As shown in Figure S6C, positive staining of Ki67 was found in FHE@exo hydrogel and exo groups (Figure S6D), while the FHE hydrogel and control groups showed very small amount of positive staining of Ki67 at both time points. Although no difference can be found by visual inspection, the quantitative data of the positively stained Ki67 numbers revealed that a significantly higher level of Ki67 was expressed in FHE@exo hydrogel group (Figure S6D) than that of the exo group. Meanwhile, the Ki67 levels of all wounds moderately decreased at day 14 when compared with day 7. At that time, the healing stage had nearly progressed from proliferation to tissue remodeling, which explained the reduced cell proliferative activities and was also confirmed by the H&E staining with less granulation tissue. Moreover, reduced proliferative activities during the late repair stage may prohibit tissue hyperplasia and lead to relatively satisfactory outcomes [47]. These results confirmed that the FHE@exo hydrogel exosomes

sustained release system enhances the cell proliferative activity of wounds sites, which promotes granulation tissue formation and further facilitates wound healing.

Blood vessels have been considered critical for tissue regeneration due to their functions of providing nutrition and oxygen for cells around wounds [48, 51]. From the *in vitro* results we can see FHE@exo hydrogel has a potent angiogenic promoting effect towards HUVECs (Figure 3). Nevertheless, whether the *in vitro* angiogenic ability of FHE@exo hydrogel would affect the angiogenesis in diabetic wounds remained unclear. Therefore, the level of alpha-smooth muscle actin ( $\alpha$ -SMA) was assessed to evaluate newly formed vessels within the regenerated tissue (Figure 6A). FHE@exo hydrogel treated diabetic wounds exhibited much higher expression of  $\alpha$ -SMA than that of the other three groups, followed by pure exosomes treated wounds. The  $\alpha$ -SMA staining in FHE and control group was very weak. Moreover, blood vessels in the FHE@exo hydrogel group appeared bigger size with lumen structure. The vessels numbers connected with smooth muscle cells was also counted according to the  $\alpha$ -SMA staining results. Consistent with the visual observation, the vessel number of FHE@exo hydrogel group in the wound site was approximately 45, while other groups showed only about 20 vessels. These data supported the *in vitro* findings of enhanced tube formation in cells treated with FHE@exo hydrogel, indicating FHE@exo hydrogel successfully promoted angiogenesis and blood vessels formation in the diabetic wounds.

From all of the above results we can see FHE@exo hydrogel, which possesses properties of self-healing, injectability, antibacterial activity, and long term pH-responsive exosomes release behavior,

has a potent effect in promoting the healing process of diabetic wounds. The efficient antibacterial ability protected diabetic wounds from infection, and none of the treated diabetic wound was infected during the experimental period. Moreover, compared with other reported hydrogels [21, 52, 53], the FHE@exo hydrogel also showed excellent cytocompatibility, angiogenic ability and can significantly accelerate the diabetic wound repair and regeneration process. Specifically, once the FHE@exo hydrogel was applied onto the diabetic wounds, the exosomes with specific miRNA and proteins also began to release from the hydrogel with a sustained profile. With these released exosomes, the angiogenesis of wounds was initiated, characterized by more newly formed vessels appearing within the wounds. Meanwhile, the proliferative activity of the involved cells was also promoted. With the increased neovascularization and proliferation, the granulation tissue formation, re-epithelialization and matrix deposition processes were accelerated, leading to shorter healing time and faster healing rates compared to exosomes treated wounds. Particularly, much less scar tissue and more skin appendages appeared in the late healing stage of diabetic wounds treated with FHE@exo hydrogel, which is probably related to the sustained release of exosomes, as fewer skin appendages can also be found in wounds treated by pure exosomes. These results remind us that the sustained release of exosomes may facilitate complete diabetic wound healing with abundant skin appendages and scarless tissue. Further studies about the specific functional component of exosomes and its related molecular mechanism in diabetic wound healing should be investigated in the near future.

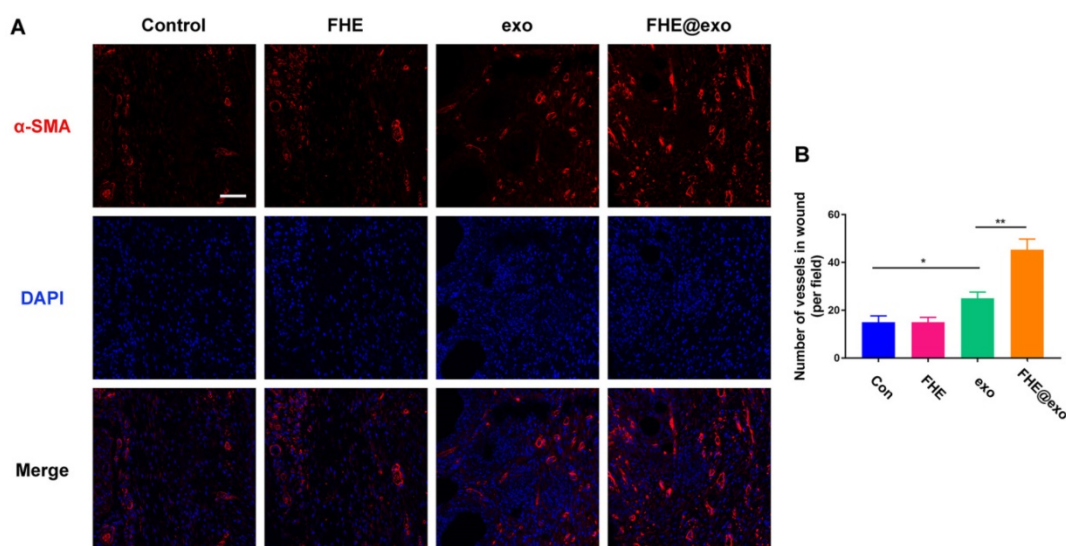


**Figure 6. Neovascularization evaluation of wounds treated by FHE@exo hydrogel.** (A) Blood vessels stained with  $\alpha$ -SMA (red) and DAPI (blue) in wound bed at days 7 postoperative. Scale bar: 20  $\mu$ m, respectively; (B) Quantitative analysis of vessels per field at 7 days after surgery corresponding to  $\alpha$ -SMA staining.

## Conclusions

In summary, a novel bioactive FHE@exo hydrogel was fabricated facilely for enhanced angiogenesis and diabetic wound healing. The FHE@exo hydrogel shows bioactive multifunctional properties including injectability, self-healing, antibacterial activity, stimuli-responsive exosomes release. The FHE@exo hydrogel significantly improved the proliferation, migration and angiogenesis of HUVECs. Further *in vivo* study confirmed that the neovascularization and cellular proliferation of the FHE@exo hydrogel treated wounds were promoted, leading to faster granulation tissue formation, re-epithelialization and collagen remodeling within wound sites; thus diabetic wound healing process was accelerated. Moreover, compared with the FHE hydrogel, exo and control groups, the appearance of abundant skin appendages and much less scar tissue in the FHE@exo hydrogel group makes FHE@exo hydrogel a highly promising therapeutic for chronic wounds and skin regeneration.

## Supplementary Material

Supplementary figures and tables.

<http://www.thno.org/v09p0065s1.pdf>

## Acknowledgement

This study was financed by National Natural Science Foundation of China (grant No. 51502237, 51802227, 51872224), Natural Science Foundation of Zhejiang Province (grant No. LGF18H150008), and Medical Health Science and Technology project of Zhejiang Province (grant No. 2019315934), Key Laboratory of Shaanxi Province for Craniofacial Precision Medicine Research, College of Stomatology, Xi'an Jiaotong University (Grant No. 2018LHM-KFKT004).

## Competing Interests

The authors have declared that no competing interest exists.

## References

- Marti-Carvajal AJ, Gluud C, Nicola S, Simancas-Racines D, Reveiz L, Oliva P, et al. Growth factors for treating diabetic foot ulcers. *Cochrane Database Syst Rev*. 2015; 10: CD008548.
- Martin P. Wound healing—aiming for perfect skin regeneration. *Science*. 1997; 276: 75-81.
- Guo S, DiPietro LA. Factors affecting wound healing. *J Dent Res*. 2010; 89: 219-29.
- Du Y, Yu M, Ge J, Ma PX, Chen X, Lei B. Development of a multifunctional platform based on strong, intrinsically photoluminescent and antimicrobial silica-poly (citrate)-based hybrid biodegradable elastomers for bone regeneration. *Adv. Funct. Mater*. 2015; 25:5016-29.
- Pop MA, Almqvist BD. Biomaterials: A potential pathway to healing chronic wounds? *Exp Dermatol*. 2017; 26: 760-3.
- Yu M, Lei B, Gao C, Yan J, Ma PX. Optimizing surface-engineered ultra-small gold nanoparticles for highly efficient miRNA delivery to enhance osteogenic differentiation of bone mesenchymal stromal cells. *Nano Res*. 2017; 10: 49-63.
- Wang Y, Han ZB, Song YP, Chao HZ. Safety of mesenchymal stem cells for clinical application. *Stem Cells Int*. 2012; 2012: 652034.
- Song M, Heo J, Chun JY, Bae HS, Kang JW, Kang H, et al. The paracrine effects of mesenchymal stem cells stimulate the regeneration capacity of endogenous stem cells in the repair of a bladder-outlet-obstruction-induced overactive bladder. *Stem Cells Dev*. 2014; 23: 654-63.
- Liang X, Ding Y, Zhang Y, Tse HF, Lian Q. Paracrine mechanisms of mesenchymal stem cell-based therapy: current status and perspectives. *Cell Transplant*. 2014; 23: 1045-59.
- Ferguson SW, Nguyen J. Exosomes as therapeutics: The implications of molecular composition and exosomal heterogeneity. *J Control Release*. 2016; 228: 179-90.
- Zhao F, Lei B, Li X, Mo Y, Wang R, Chen D, et al. Promoting *in vivo* early angiogenesis with sub-micrometer strontium-contained bioactive microspheres through modulating macrophage phenotypes. *Biomaterials*. 2018; 178: 36-47.
- Zhang J, Guan J, Niu X, Hu G, Guo S, Li Q, et al. Exosomes released from human induced pluripotent stem cells-derived MSCs facilitate cutaneous wound healing by promoting collagen synthesis and angiogenesis. *J Transl Med*. 2015; 13: 49.
- Zhang B, Wang M, Gong A, Zhang X, Wu X, Zhu Y, et al. HucMSC-exosome mediated-Wnt4 signaling is required for cutaneous wound healing. *Stem Cells*. 2015; 33: 2158-68.
- Guo SC, Tao SC, Yin WJ, Qi X, Yuan T, Zhang CQ. Exosomes derived from platelet-rich plasma promote the re-epithelization of chronic cutaneous wounds via activation of YAP in a diabetic rat model. *Theranostics*. 2017; 7: 81-96.
- Liu X, Yang Y, Li Y, Niu X, Zhao B, Wang Y, et al. Integration of stem cell-derived exosomes with *in situ* hydrogel glue as a promising tissue patch for articular cartilage regeneration. *Nanoscale*. 2017; 9: 4430-8.
- Xi Y, Ge J, Guo Y, Lei B, Ma PX. Biomimetic Elastomeric Polypeptide-Based Nanofibrous Matrix for Overcoming Multidrug-Resistant Bacteria and Enhancing Full-Thickness Wound Healing/Skin Regeneration. *ACS Nano*. 2018;12:10772-84.
- Sharifzadeh G, Hosseinkhani H. Biomolecule-responsive hydrogels in medicine. *Adv Healthc Mater*. 2017; 6: 1700801.
- Annabi N, Rana D, Shirzaei Sani E, Portillo-Lara R, Gifford JL, Fares MM, et al. Engineering a sprayable and elastic hydrogel adhesive with antimicrobial properties for wound healing. *Biomaterials*. 2017; 139: 229-43.
- Taylor DL, Marc IHP. Self-healing hydrogels. *Adv Mater*. 2016; 28: 9060-93.
- Li Y, Wang X, Fu YN, Wei Y, Zhao L, Tao L. Self-adapting hydrogel to improve the therapeutic effect in wound-healing. *ACS Appl Mater Interfaces*. 2018; 10: 26046-55.
- Mao C, Xiang Y, Liu X, Cui Z, Yang X, Yeung KWK, et al. Photo-inspired antibacterial activity and wound healing acceleration by hydrogel embedded with Ag/AgCl/ZnO nanostructures. *ACS Nano*. 2017; 11: 9010-21.
- Xie X, Mao C, Liu X, Zhang Y, Cui Z, Yang X, et al. Synergistic bacteria killing through photodynamic and physical actions of Graphene Oxide/Ag/Collagen coating. *ACS Appl Mater Interfaces*. 2017; 9: 26417-28.
- Xie X, Mao C, Liu X, Tan L, Cui Z, Yang X, et al. Tuning the bandgap of photo-sensitive Polydopamine/Ag<sub>3</sub>PO<sub>4</sub>/Graphene Oxide coating for rapid, noninvasive disinfection of implants. *ACS Cent Sci*. 2018; 4: 724-38.
- Tan L, Li J, Liu X, Cui Z, Yang X, Zhu S, et al. Rapid biofilm eradication on bone implants near-infrared light. *Adv Mater*. 2018; 30: e1801808.
- Li J, Tan L, Liu X, Cui Z, Yang X, Yeung KWK, et al. Balancing bacteria-osteoblast competition through selective physical puncture and biofunctionalization of ZnO/Polydopamine/Arginine-Glycine-Aspartic Acid-Cysteine nanorods. *ACS Nano*. 2017; 11: 11250-63.
- Boateng J, Catanzano O. Advanced therapeutic dressings for effective wound healing—a review. *J Pharm Sci*. 2015; 104: 3653-80.
- Liao J, Jia Y, Wang B, Shi K, Qian Z. Injectable hybrid poly( $\epsilon$ -caprolactone)-b-poly(ethylene glycol)-b-poly( $\epsilon$ -caprolactone) porous microspheres/alginate hydrogel cross-linked by calcium gluconate crystals deposited in the pores of microspheres improved skin wound healing. *ACS Biomater Sci Eng*. 2018; 4: 1029-36.
- Zheng Y, Liang Y, Zhang D, Sun X, Liang L, Li J, et al. Gelatin-based hydrogels blended with gellan as an injectable wound dressing. *ACS Omega*. 2018; 3: 4766-75.
- Ge J, Liu K, Niu W, Chen M, Wang M, Xue Y, et al. Gold and gold-silver alloy nanoparticles enhance the myogenic differentiation of myoblasts through p38 MAPK signaling pathway and promote *in vivo* skeletal muscle regeneration. *Biomaterials*. 2018; 175: 19-29.
- Wang M, Guo Y, Yu M, Ma PX, Mao C, Lei B. Photoluminescent and biodegradable polycitrate-polyethylene glycol-poly(ethyleneimine) polymers as highly biocompatible and efficient vectors for bioimaging-guided siRNA and miRNA delivery. *Acta Biomater*. 2017;54:69-80.
- Zhou L, Xi Y, Chen M, Niu W, Wang M, Ma P X, et al. A highly antibacterial polymeric hybrid micelle with efficiently targeted anticancer siRNA delivery and anti-infection *in vitro/in vivo*. *Nanoscale*. 2018; 10: 17304-17.
- Zhou L, Xi Y, Yu M, Wang M, Guo Y, Li P, et al. Highly antibacterial polypeptide-based amphiphilic copolymers as multifunctional non-viral vectors for enhanced intracellular siRNA delivery and anti-infection. *Acta Biomater*. 2017; 58: 90-101.

33. Zhou Y, Nie W, Zhao J, Yuan X. Rapidly in situ forming adhesive hydrogel based on a PEG-maleimide modified polypeptide through Michael addition. *J Mater Sci Mater Med.* 2013; 24: 2277-86.
34. Zhang K, Zhao X, Chen X, Wei Y, Du W, Wang Y, et al. Enhanced therapeutic effects of mesenchymal stem cell-derived exosomes with an injectable hydrogel for hindlimb ischemia treatment. *ACS Appl Mater Interfaces.* 2018; 10: 30081-91.
35. Shi Q, Qian Z, Liu D, Sun J, Wang X, Liu H, et al. GMSC-derived exosomes Combined with a chitosan/silk hydrogel sponge accelerates wound healing in a diabetic rat skin defect model. *Front Physiol.* 2017; 8: 904.
36. Tan A, Rajadas J, Seifalian AM. Exosomes as nano-theranostic delivery platforms for gene therapy. *Adv Drug Deliver Rev.* 2013; 65: 357-67.
37. Wei Z, Yang JH, Zhou J, Xu F, Zrinyi M, Dussault PH, et al. Self-healing gels based on constitutional dynamic chemistry and their potential applications. *Chem Soc Rev.* 2014; 43: 8114-31.
38. Lei ZQ, Xie P, Rong MZ, Zhang MQ. Catalyst-free dynamic exchange of aromatic Schiff base bonds and its application to self-healing and remodeling of crosslinked polymer. *J Mater Chem A.* 2015; 3: 19662-8.
39. De Jong OG, Van Balkom BW, Schiffelers RM, Bouten CV, Verhaar MC. Extracellular vesicles: potential roles in regenerative medicine. *Front Immunol.* 2014; 5: 608.
40. Crivelli B, Chlapanidas T, Perteghella S, Lucarelli E, Pascucci L, Brini AT, et al. Mesenchymal stem/stromal cell extracellular vesicles: From active principle to next generation drug delivery system. *J Control Release.* 2017; 262: 104-17.
41. Du Y, Ge J, Li Y, Ma P X, Lei B. Biomimetic elastomeric, conductive and biodegradable polycitrate-based nanocomposites for guiding myogenic differentiation and skeletal muscle regeneration. *Biomaterials.* 2018; 157: 40-50.
42. Liang X, Zhang L, Wang S, Han Q, Zhao RC. Exosomes secreted by mesenchymal stem cells promote endothelial cell angiogenesis by transferring miR-125a. *J Cell Sci.* 2016; 129: 2182-9.
43. Li M, Ke Q, Tao S, Guo S, Rui B, Guo Y. Fabrication of hydroxyapatite/chitosan composite hydrogels loaded with exosomes derived from miR-126-3p overexpressed synovial mesenchymal stem cells for diabetic chronic wound healing. *J Mater Chem B.* 2016; 4: 6830-41.
44. Epstein FH, Singer AJ, Clark RAF. Cutaneous wound healing. *N Engl J Med.* 1999; 341: 738-46.
45. Wu J, Zhu J, He C, Xiao Z, Ye J, Li Y, et al. Comparative study of heparin-poloxamer hydrogel modified bFGF and aFGF for in vivo wound healing efficiency. *ACS Appl Mater Interfaces.* 2016; 8: 18710-21.
46. Gao W, Jin W, Li X, Wan L, Wang C, Lin C, et al. A highly bioactive bone extracellular matrix-biomimetic nanofibrous system with rapid angiogenesis promotes diabetic wound healing. *J. Mater. Chem. B* 2017; 5:7285-7296.
47. Liu X, Ma L, Liang J, Zhang B, Teng J, Gao C. RNAi functionalized collagen-chitosan/silicone membrane bilayer dermal equivalent for full-thickness skin regeneration with inhibited scarring. *Biomaterials.* 2013; 34: 2038-48.
48. Wang C, Wang Q, Gao W, Zhang Z, Lou Y, Jin H, et al. Highly efficient local delivery of endothelial progenitor cells significantly potentiates angiogenesis and full-thickness wound healing. *Acta Biomater.* 2018; 69: 156-69.
49. Liu X, Ma L, Liang J, Zhang B, Teng J, Gao C. RNAi functionalized collagen-chitosan/silicone membrane bilayer dermal equivalent for full-thickness skin regeneration with inhibited scarring. *Biomaterials.* 2013; 34: 2038-48.
50. Xu H, Lv F, Zhang Y, Yi Z, Ke Q, Wu C, et al. Hierarchically micro-patterned nanofibrous scaffolds with a nanosized bio-glass surface for accelerating wound healing. *Nanoscale.* 2015; 7: 18446-52.
51. Gurtner GC, Werner S, Barrandon Y, Longaker MT. Wound repair and regeneration. *Nature.* 2008; 453: 314-21.
52. Kurokawa I, Mizutani H, Kusumoto K, Nishijima S, Tsujita-Kyutoku M, Shikata N, et al. Cytokeratin, filaggrin, and p63 expression in reepithelialization during human cutaneous wound healing. *Wound Repair Regen.* 2006; 14: 38-45.
53. Weihs AM, Fuchs C, Teuschl AH, Hartinger J, Slezak P, Mittermayr R, et al. Shock wave treatment enhances cell proliferation and improves wound healing by ATP release-coupled extracellular signal-regulated kinase (ERK) activation. *J Biol Chem.* 2014; 289: 27090-104.
54. Nomi M, Atala A, De Coppi P, Soker S. Principles of neovascularization for tissue engineering. *Mol Aspects Med.* 2002; 23: 463-83.
55. Mao C, Xiang Y, Liu X, Cui Z, Yang X, Li Z, et al. Repeatable photodynamic therapy with triggered signaling pathways of fibroblast cell proliferation and differentiation to promote bacteria-accompanied wound healing. *ACS Nano.* 2018; 12: 1747-59.
56. Li M, Liu X, Tan L, Cui Z, Yang X, Li Z, et al. Noninvasive rapid bacteria-killing and acceleration of wound healing through photothermal/photodynamic/copper ion synergistic action of a hybrid hydrogel. *Biomater Sci.* 2018; 6: 2110-21.